Materials Physics and Mechanics. 2023;51(4): 85-95
Research article
http://dx.doi.org/10.18149/MPM.5142023_8

Submitted: May 16, 2023
Approved: May 23, 2023
Accepted: June 28, 2023

# Spin transistor effect in edge channels of silicon nanosandwiches

**L.E. Klyachkin ✉, N.T. Bagraev, A.M. Malyarenko**

Ioffe Institute, St. Petersburg, Russia

✉ leonid.klyachkin@gmail.com

**Abstract.** The conductance dependences of the edge channels of silicon nanosandwich structures (SNS) on the vertical gate voltage $V_g$ are studied. The experiments are carried out in such a range of $V_g$, in which the two-dimensional density of holes $p_{2D}$ is stable that made it possible to avoid the changes of the Fermi level position and thereby to unambiguously identify the Aharonov–Casher oscillations. The effect of a spin field-effect transistor at a high temperature ($T$ = 77 K) is demonstrated, which manifests itself in the form of Aharonov–Casher oscillations of longitudinal conductance depending on $V_g$, which controls the Bychkov–Rashba spin-orbit interaction. This experiment became possible due to the high degree of spin polarization of holes and the long spin-lattice relaxation time because of the extremely small width of the silicon quantum well and the narrowness of its edge channels, which is ensured by the properties of the negative-U-barriers limiting them effectively decreasing the electron-electron interaction.
**Keywords:** silicon nanosandwich; edge channel; Aharonov–Casher oscillations; Bychkov–Rashba spin-orbit interaction; spin field-effect transistor

***Acknowledgements***. *The work was financed within the framework of the State task on the topic 0040-2019-0017 "Interatomic and atomic-molecular interactions in gases and condensed matter; quantum magnetometry and multiphoton laser spectroscopy".*

**Citation:** Klyachkin LE, Bagraev NT, Malyarenko AM. Spin transistor effect in edge channels of silicon nanosandwiches. *Materials Physics and Mechanics*. 2023;51(4): 85-95. DOI: 10.18149/MPM.5142023_8.

## Introduction

In the last decades of the 20th century, progress in the field of semiconductor nanotechnologies led to the creation of structures with quasi-one-dimensional (1D) conducting channels with the length less than the inelastic scattering length [1,2], due to which the ballistic transfer of single carriers occurs in them and macroscopic quantum phenomena are observed.

Therefore, such channels provide conditions for spin interference of single carriers due to spontaneous spin polarization of a quasi 1D carrier gas in a zero magnetic field [3,4] and Bychkov–Rashba strong spin-orbit interaction (SOI) [5].

Obviously, such semiconductor nanostructures are promising for solving various problems of high-temperature nano- and optoelectronics, especially for the experimental implementation of electron-wave analogues of electro-optical modulators. The most striking proposal consists in creating a spin field-effect transistor (SFET) [6–10].

The current modulation in the SFET structure occurs due to quantum interference effects, namely, due to the spin precession caused by Bychkov–Rashba SOI in an ultra-narrow quantum well, which is the main element of the field-effect transistor. At the same

time, magnetic contacts, which play the role of source and drain, are preferentially used for injection and detection of certain spin orientations (Fig. 1) [6]. In the SFET structure, the source and drain, which are also a polarizer and analyzer, can be made of a ferromagnet, such as iron. At the Fermi level in such materials, the density of states of an electron with one spin orientation greatly exceeds the density of states with another spin orientation, so that the contact preferentially injects and detects electrons with a certain spin direction. The spin polarization of the current, reaching ~50 % in this case, was experimentally demonstrated using contacts made of permalloy (a magnetically soft alloy of Ni with Fe) [11,12]. A contact magnetized in the *x* direction preferentially emits and detects spin-polarized electrons along the positive *x*-axis, which is represented as a linear combination of positive *z*-polarized and negative *z*-polarized electrons.

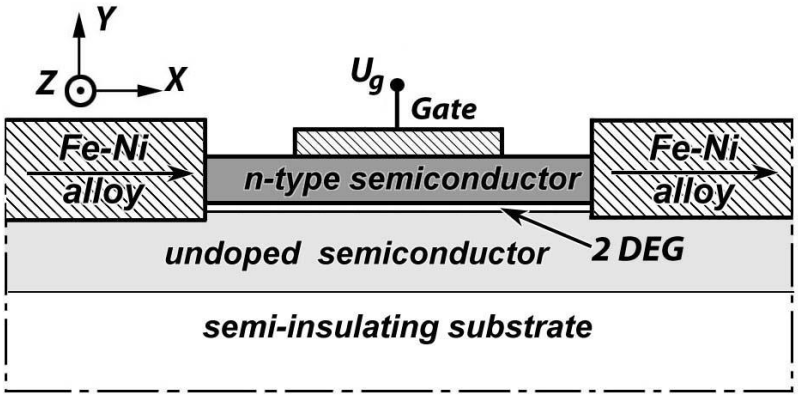


**Fig. 1.** Diagram of a spin field-effect transistor

By analogy with an electro-optical material, the differential phase shift introduced between +*z* polarized and –*z* polarized electrons can be controlled by the vertical gate voltage of the FET, which controls the SOI value in the quantum well [6]. It is assumed that the dominant mechanism of spin energy splitting between electrons with spins up and down in a zero magnetic field, as indicated above, is the Bychkov–Rashba term [13], taken into account in the effective-mass Hamiltonian [6]:

$$H_R = \alpha\left(\sigma_z k_x - \sigma_x k_z\right), \quad (1)$$

where $\alpha$ is the Rashba SOI parameter, which depending on the type of quantum well conductance is determined by the characteristics of the conduction band or valence band [13–15]. This term is a consequence of the presence of an electric field perpendicular to the plane of the quantum well or the interface of a single heterojunction. Other mechanisms of spin splitting in a zero magnetic field, for example, due to the influence of the inversion center, can also contribute [16]. However, if the quantum well is formed inside the p-n junction, their contribution to the SOI value is much less than the Bychkov–Rashba term. It is easy to see that the Bychkov–Rashba term leads to the fact that +*z* and –*z* polarized electrons have the same energy and different wave vectors $k_1$ and $k_2$. Moreover, if we consider an electron moving in the *x* direction with $k_z=0$ and $k_x\neq0$, the Bychkov–Rashba term $H_R$ is equal to $\alpha\sigma_z k_x$, which increases the energy of +*z* polarized electrons by $\alpha k_x$ and, respectively, reduces the energy of –*z* polarized electrons by the same value. A similar change in energy can be achieved if the electron were in a magnetic field $B_z$ proportional to $k_x$ ($\alpha k_x$ -> $\mu_B B_z$, where $\mu_B$ is the Bohr magneton).

This energy difference for $+z$ polarized and $-z$ polarized electrons can lead, under the condition of their transport along the $x$ direction, to a differential phase shift, $\Delta\theta$, proportional to the Bychkov–Rashba SOI parameter, the value of which can be varied using the vertical gate voltage

$$E(+z\ pol.) = \hbar^2 k^2_{x1}/2m^* - \alpha k_{x1}, \quad (2)$$

$$E(-z\ pol.) = \hbar^2 k^2_{x2}/2m^* + \alpha k_{x2}. \quad (3)$$

$$\Delta\theta = (k_{x1} - k_{x2})L = 2m^*\alpha L/\hbar^2. \quad (4)$$

Thus, within the framework of the described field-effect transistor structure, current modulation can occur due to spin precession under SOI conditions, thereby identifying the effect of SFET depending on the vertical gate voltage.

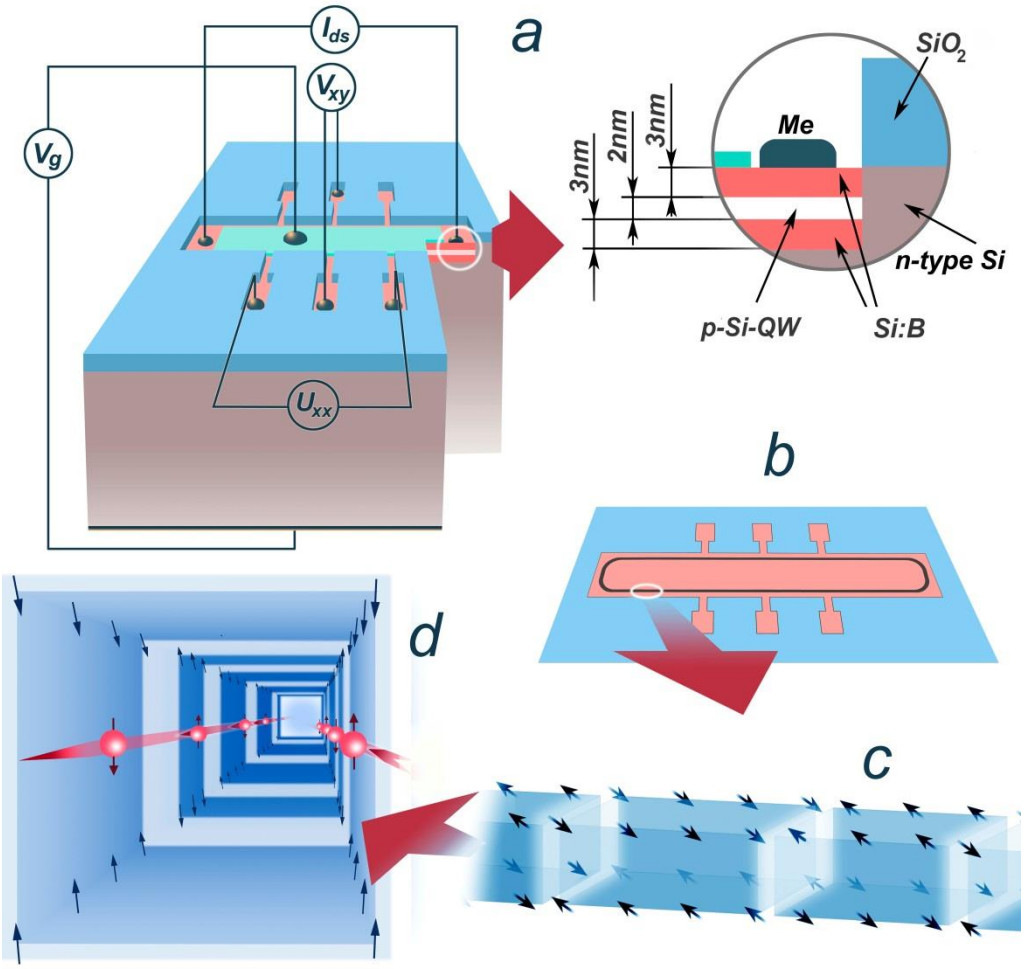


**Fig. 2.** Experimental SNS made in Hall geometry to demonstrate the SFET effect (a). Topological edge channel of the SNS (b), in which single charge carriers occupy its separate areas, pixels (c). Polarized carriers are transported along opposite pixel walls of the edge channel (d)

The discovery of spin interference in 1D channels contributed to the development of spintronic devices based on the phenomena of spin interference, which are able to demonstrate SFET characteristics even without ferromagnetic electrodes and external magnetic fields in the presence of spin polarization in low-dimensional systems [13,17]. Moreover, it is advisable to create spintronic devices based on topological insulators and superconductors with a control vertical gate, which, in addition to the geometric Berry phase, provides a phase shift between the transmission amplitudes for carriers moving clockwise and counterclockwise [13] (see Fig. 2 ). This phase shift leads to the observation of Aharonov–

Casher (AC) conductance oscillations, measured by varying the voltage on the vertical gate that controls the transport of single carriers in quasi-one-dimensional channels, even in the absence of an external magnetic field and magnetic electrodes responsible for obtaining and recording the spin polarization of carriers. However, changes in the carrier density that accompany the application of a voltage on a vertical gate can also cause conductance oscillations resulting from changes in the value of the Fermi wave vector, although they are similar in appearance to oscillations in the AC conductance [18,19].

Nevertheless, the unambiguous identification of AC conductance oscillations when controlling the transport of single carriers using a change in the vertical gate, and, consequently, the demonstration of the SFET effect, turned out to be possible when using a silicon nanosandwich structure (SNS) for this purpose.

**Methods**

In this work, to determine the contribution of the AC effect to the conductance oscillations and to demonstrate the SFET effect, we use an SNS with a diffusion profile depth of 8 nm (according to SIMS data), containing a single quantum well about 2 nm wide. The well is bounded by two δ-barriers consisting of $B^+$-$B^-$ dipoles with negative correlation energy (negative-U), formed due to the interconnectedness of the electron-vibrational and electron-electron interactions [20]. A similar effect occurs at an ultrahigh concentration of boron dopant in δ-barriers (about 5 $10^{21}$ $cm^{-3}$) [20]. The SNS was made in the Hall geometry and equipped with an additional control electrode, which is used as a vertical gate, to which voltage $V_g$ is applied (Fig. 2(a)). The vertical gate electrode was formed on the surface of a thin (about 20 nm) gate insulator $SiO_2$ layer preliminarily deposited on the SNS by the plasma-chemical method.

Previous studies of the de Haas–van Alphen (DHVA), Shubnikov–de Haas (SdH) and quantum Hall effects (QHE) [21] showed that in this experimental SNS, the two-dimensional concentration $p_{2D}$ of single charge carriers in a quantum well bounded by a negative-U δ-barriers is $3 \cdot 10^{13}$ $m^{-2}$. Their behavior is characterized by a long relaxation time and a low value of the effective mass ($m^* < 10^{-3} m_0$) [22].

In addition, it was experimentally demonstrated that the transport of single charge carriers in SNS occurs in topological edge channels (ECs) (Fig. 2(b)), formed in the SNS quantum well by chains of negative-U boron dipole centers [21]. It was shown that it is precisely due to such chains of negative-U dipoles, which form and limit ECs, that conditions are created for the effective suppression of the electron-electron interaction (EEI) in ECs, which, in turn, made it possible to observe the above macroscopic quantum effects in SNS at high temperatures up to the room one [21].

The cross-sectional area of the ECs of the SNS under study is 2×2 nm, since 2 nm is the characteristic distance between the negative-U δ-barriers that form them. Previous experiments showed that the EC of the studied SNS consists of regions of single carrier interference, the length of which is approximately 16 μm, taking into account the value of the 2D density of single carriers determined from Hall measurements [21]. That is, each region of the EC, in which a single carrier (“pixel”) is located, consists of layers containing negative-U boron dipoles with an area of $S_{pixel} = 16 \times 2$ $nm^2$, along which the carrier tunneling occurs (Fig. 2(c)). In this case, the resistance of a single carrier in a pixel is quantized and amounts to $n(h/e^2)$ [21,23].

The spin polarization of single carriers in ECs of such SNSs was observed experimentally, and it was shown that ECs are paired, and the carriers in them have opposite spin orientations [4,21]. Obviously, in such ECs, single carriers have the ability to interfere both in the entire EC (or part of it) and inside a single pixel, since carriers

with different spins move towards each other on opposite sides of the pixel under the action of the field (Fig. 2(d)) [4].

To demonstrate the SFET effect, such an SNS has a number of advantages. First, due to the built-in p-n junction in the QW, the electric field sharply increases, which contributes to an increase in the Bychkov–Rashba SOI. Second, as noted above, the EEI inside the EC is leveled due to the interaction of single carriers with negative-U dipole boron centers, which makes it possible to study the macroscopic phenomena of quantum interference at high temperatures [22]. In addition, it should be noted that, in the SNSs under study, the carriers in ECs are holes, which exhibit a stronger SOI compared to electrons [16].

In order to demonstrate the SFET effect, it is necessary to study the conductance of the SNS EC experimentally by varying the vertical gate voltage $V_g$, since in this case it becomes possible to control the Bychkov–Rashba SOI and, thus, the spin polarization of holes in the EC. However, when performing experiments, it should be taken into account that varying the value of $V_g$ leads to a change in the concentration and mobility of 2D holes in the QW. This, at first glance, may interfere with the unambiguous identification of the AC conductance oscillations caused by the Bychkov–Rashba SOI, since other effects, such as the influence of the position of the Fermi level, also cause conductance oscillations due to changes in the density and mobility of 2D holes.

The concentration of 2D holes and their mobility in a silicon QW were determined from Hall measurements (Fig. 3) [22]. The initial value of the density of 2D holes $p_{2D} = 4 \cdot 10^{13}$ m$^{-2}$ ($V_g = 0$) was controlled by an order of magnitude, between $5 \cdot 10^{12}$ m$^{-2}$ and $9 \cdot 10^{13}$ m$^{-2}$, by shifting on the vertical gate through the insulator layer, which performs the function $p^+$-n junction offsets. It was shown that in the vertical gate voltage range between 150 and 400 mV, $p_{2D}$ is practically independent of $V_g$. Therefore, this $V_g$ range can be used to identify AC oscillations caused by the Bychkov–Rashba SOI.

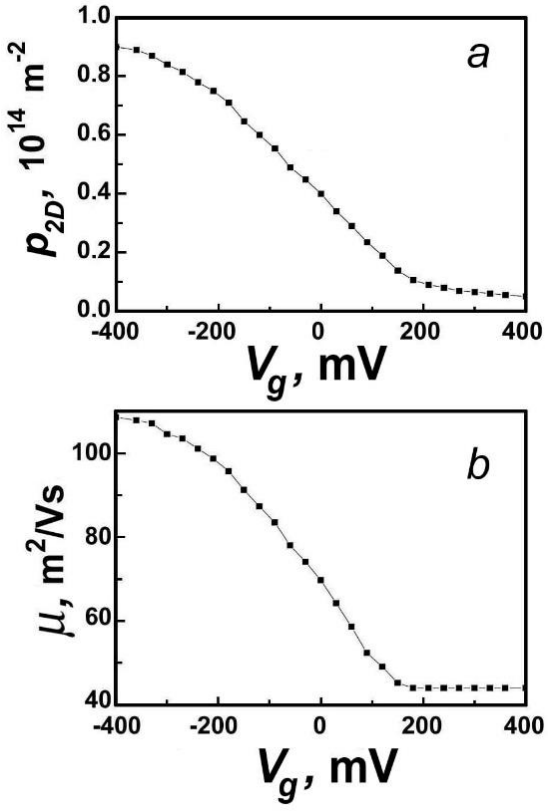


**Fig. 3.** Density (a) and mobility (b) of a 2D hole gas as a function of vertical gate voltage obtained from measurements of the longitudinal and Hall stresses in the SNS on an n-type Si(100) surface. T=77 K

The experimental conductance dependences on $V_g$ displacement on the vertical gate of the SNS structure made in the Hall geometry (Fig. 2(a)) were obtained at a liquid nitrogen temperature of 77 K. In the experiment, the dependence $U_{xx} = f(V_g)$ was recorded, after which the dependence was calculated $G = f(V_g)$. The measurements were carried out on an experimental bench using Keithley 2182A nanovoltmeters, a Keithley 2010 multimeter, a Keithley 6517A electrometer, and a Keithley 6221 current source. The vertical gate was biased from an independent power source galvanically isolated from the measuring circuit.

As seen in Fig. 2(a), the Hall geometry of the SNS determines its symmetry. For this reason, this article presents the experimental results of measuring $U_{xx}$ for only one pair of the contacts, since $U_{xx}$ measurements on the opposite pair of contacts give equivalent results due to the symmetry of the SNS geometry.

**Results**

To determine the contribution of the Bychkov–Rashba SOI to the conductance (transmission) of the SNS EC structure, the dependence $U_{xx} = f(V_g)$ was studied under conditions of varying $V_g$ followed by the calculation of the dependence $\Delta G = f(V_g)$. Its analysis made it possible to reveal the spin splitting of holes 44 meV in 1D gas (Fig. 4).

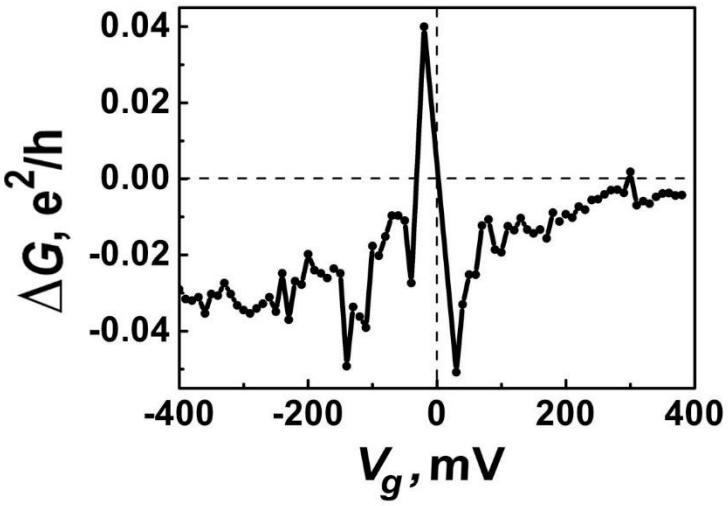


**Fig. 4.** Conductance change $\Delta G$ as a function of the vertical gate voltage applied to the SNS edge channel. T=77 K

The value of the spin splitting 44 meV corresponds to the value of the spin-orbit interaction in the valence band. These data seem to indicate spontaneous spin polarization of heavy holes in the 1D channel due to effective quenching of the kinetic energy by the exchange energy of carriers [4].

Experimental studies of the dependences $\Delta G = f(V_g)$ were carried out in the range $V_g$ = 150–400 mV, which makes it possible to unambiguously identify AC oscillations (Fig. 5) caused by the Bychkov–Rashba SOI.

Changes in the phase of the AC oscillations shown in Fig. 5 are apparently caused by the elastic scattering of heavy holes on the quantum point contact inside the EC of SNS. The phase shifts calculated within this model depend on the parameter α determined by the effective magnetic field created by the Bychkov–Rashba SOI [5,6,13–15,18,19,24,25]:

$$\mathbf{B}_{eff} = \frac{\alpha}{g_B \mu_B}\left[\mathbf{k} \times \mathbf{e}_z\right], \quad (5)$$

which affects the conductance modulation [14,15], which is consistent with the oscillations of the AC conductance (Fig. 5). Note that the Bychkov–Rashba SOI in 2D systems cubically depends on the wave vector. However, in a 1D system, it is necessary to average the wave vector components perpendicular to the 1D channel axis. Therefore, the resulting Bychkov–Rashba SOI for 1D hole systems depends linearly on the wave number, as does the Dresselhaus SOI in 1D electron systems [16].

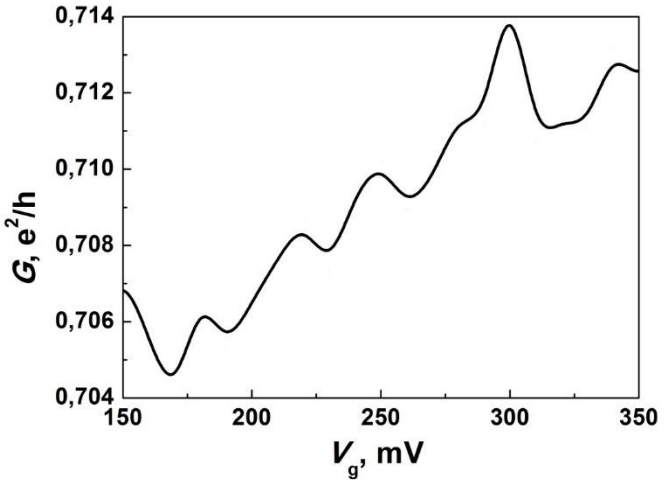


**Fig. 5.** The Aharonov–Casher conductance oscillations in the edge channel of the SNS. T=77 K

The oscillation period of the AC conductance ($\Delta V_g$), which is determined by the quantum transport of holes through the quantum point contact, can be estimated from the following relations [14,15]:

$$\Delta V_g \approx \frac{\mathrm{h}^2 d^2 l}{3\pi^2 R m_{eff} \beta_{hh}}, \tag{6}$$

where $l$ is the characteristic length, which provides proportionality between the vertical gate voltage $V_g$ and the electric field, $V_g = Ez\ l$, and is determined by the thickness of the n-type Si(100) plate, $l$ = 300 nm; $d$ is the diameter of the edge channel, 2 nm; $R$ is the effective average pixel radius, the value of which can be controlled by changing the 2D concentration $p_{2D}$ by varying the value of $V_g$. As mentioned above, to identify the Bychkov–Rashba SOI in these experiments, it is necessary to use a range of $V_g$ values in which the $p_{2D}$ value remains practically unchanged. In this case, the value $R \approx 2500$ nm. The value of $\beta_{hh}$ is determined by the Bychkov–Rashba parameter $\alpha$:

$$\alpha_{hh} = -3\beta_{hh}\left\langle k_r^2 \right\rangle E_z, \tag{7}$$

$$\beta_{hh} = a\left(\gamma_2 + \gamma_3\right)\gamma_3 \left[ \frac{1}{\varepsilon_1^{hh} - \varepsilon_1^{lh}} \left( \frac{1}{\varepsilon_1^{hh} - \varepsilon_2^{lh}} - \frac{1}{\varepsilon_1^{hh} - \varepsilon_2^{hh}} \right) + \frac{1}{\left(\varepsilon_1^{hh} - \varepsilon_2^{lh}\right)\left(\varepsilon_1^{hh} - \varepsilon_2^{hh}\right)} \right] \frac{e\mathrm{h}^4}{m_{eff}^2} \approx$$
$$\approx 0.02 \left[ \frac{1}{\varepsilon_1^{hh} - \varepsilon_1^{lh}} \left( \frac{1}{\varepsilon_1^{hh} - \varepsilon_2^{lh}} - \frac{1}{\varepsilon_1^{hh} - \varepsilon_2^{hh}} \right) + \frac{1}{\left(\varepsilon_1^{hh} - \varepsilon_2^{lh}\right)\left(\varepsilon_1^{hh} - \varepsilon_2^{hh}\right)} \right] \frac{e\mathrm{h}^4}{m_{eff}^2}, \tag{8}$$

where the value $\left\langle k_r^2 \right\rangle$ is approximately estimated as $\left\langle k_r^2 \right\rangle \approx \pi^2 / d^2$; $d$ is the diameter of the edge channel $a = \frac{64}{9\pi^2} \approx 0.7$ [11]; $\gamma_2 = -0.18$, $\gamma_3 = -0.1$ are Luttinger parameters for

silicon [26]; $\varepsilon_{1,2}^{lh,hh}$ are the energies of the light and heavy holes in the QW, where the subscript indicates the number of subbands, and the superscript corresponds to a light or heavy hole. Previously, in [27], the results of optical studies were presented, which made it possible to determine the energies of both light and heavy holes in the silicon QW of the SNS used in these experiments: $\varepsilon_1^{hh} = 90meV$; $\varepsilon_1^{lh} = 114meV$; $\varepsilon_2^{hh} = 307meV$; $\varepsilon_2^{lh} = 476meV$.

A detailed analysis of the AC conductance oscillations, taking into account the dependence of the 2D hole density $p_{2D}$ on the vertical gate voltage $V_g$ [22], made it possible to determine the values of the effective mass of heavy holes $m^*$ depending on the value of $p_{2D}$ at the level of $m^* = 10^{-4} - 10^{-3}$ $m_0$. Note that such a low value of m*, which is largely a consequence of negative-U δ-barriers limiting the SNS EC, is an important circumstance for the detection of spin-dependent transport at high temperatures (77 K). This makes the properties of SNS similar to those of graphene [28].

Thus, due to the spin polarization of carriers in the edge channels of the SNS, caused by the Bychkov–Rashba SOI, it becomes possible to create a SFET without special ferromagnetic electrodes or any external magnetic fields, while the channel conductance between the source-drain contacts is controlled only by voltage changes at the vertical gate $V_g$ (Fig. 6).

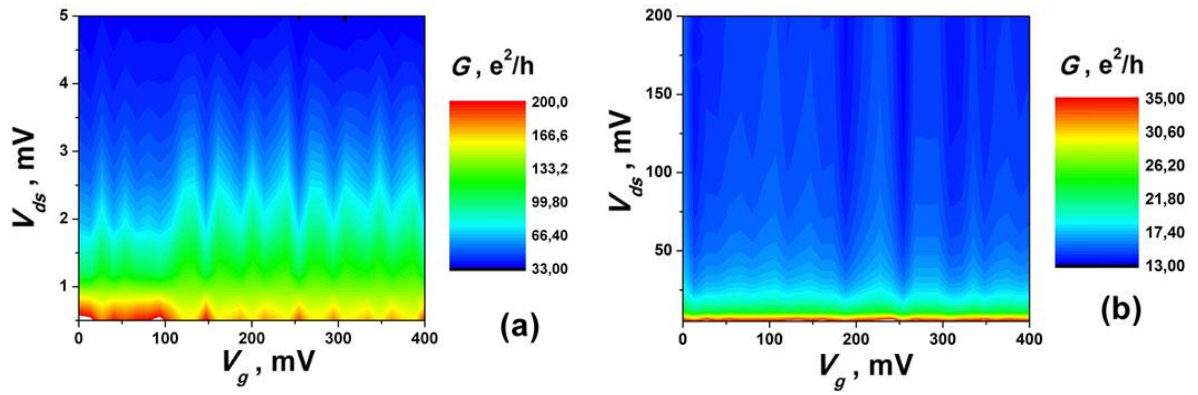


**Fig. 6.** Diagrams of AC conductance oscillations in a zero magnetic field as a function of the vertical gate voltage $V_g$, which controls the SOI value, and the source-drain voltage $V_{ds}$ applied to the SNS-based SFET. T=77 K

Oscillations of the AC conductance in the dependence of $G = f(V_g)$, which determine the SFET effect, are described using the relations obtained under the condition of effective backscattering at the quantum point contact [25,29]:

$$G = 2\frac{e^2}{h}\left(1 - |B|^2\right), \tag{9}$$

where

$$B(\alpha, E, \Phi) = \frac{\sin^2\left(\frac{\pi m \alpha a}{\hbar^2} + \frac{e\Phi}{2hc}\right)}{1 - \exp\left(2\pi i a \sqrt{\left(\frac{m}{\hbar^2}\right)\left(\frac{m\alpha^2}{\hbar^2} + 2E\right)}\right)\cos^2\left(\frac{\pi m \alpha a}{\hbar^2} + \frac{e\Phi}{2hc}\right)}. \tag{10}$$

The value of parameter $a$ is determined by the Hall geometry of the contacts and the dimensions of the device structure. In the case of SNS $a=(a_{xx} \cdot a_{xy})^{1/2}$; where $a_{xx}$ and $a_{xy}$ are the distance between contacts XX and XY, $a_{xx}$ =2 mm, $a_{xy}$=0.2 mm. These dependences describe conductance oscillations with greater accuracy when varying the value of $V_g$ (also in the case

of a nonzero external magnetic field ($\Phi=BS$)) than a more simplified relation that does not take into account its influence [24]:

$$G=\frac{e^2}{h}\left[1+\cos\left(2\pi a\frac{\alpha m}{\mathrm{h}^2}\right)\right]. \quad (11)$$

The behavior of the AC oscillations shows that the obtained structure is indeed the SFET structure. It should be noted that the magnitude of the amplitude of conductance oscillations at low values of the source-drain voltage ($V_{ds}$) is significantly less than the magnitude of the conductance quantum $e^2/h$, which may be a consequence of weak localization at a low kinetic energy of low density carriers in the EC (Fig. 5). With an increase in the kinetic energy of carriers in the optimal voltage range $V_{ds}$, the magnitude of the conductance oscillation amplitude corresponds to the conductance value $e^2/h$ (Fig. 6(a)). With a further increase in $V_{ds}$, quenching of conductance oscillations is observed (Fig. 6(b)) as a result of heating of two-dimensional holes and, consequently, a decrease in their spin-lattice relaxation time.

The presented dependences of the conductance (transmission) of the edge channels of the silicon SNS QW $G=f(V_{ds},V_g)$, demonstrating the SFET effect, in fact, are a variant of the AC effect [13,29].

Note that the observation of AC oscillations in hole conduction, illustrating the SFET effect at a high temperature (T = 77 K), became possible due to the high degree of spin polarization of holes and the large time of their spin relaxation. This, in turn, is due to the extremely small width of the silicon QW [30], the narrowness of its ECs, and effective suppression of EEI in them, which is ensured by the properties of the negative-U δ-barriers limiting them.

## Conclusions

The paper presents experimental research into dependences of the conductance of the SNS edge channels on the vertical gate voltage $V_g$. The studies were carried out in such a range of $V_g$, in which the two-dimensional concentration of holes $p_{2D}$ in the QW is practically independent of the $V_g$ value, which makes it possible to avoid the influence of a change in the position of the Fermi level. Therefore, it was possible to avoid the influence of the $p_{2D}$ change effect in the experiments and ensure unambiguous identification of the AC oscillations.

The effect of a spin transistor at a high temperature (T=77 K) was registered, which manifests itself in the form of the AC oscillations of longitudinal conductance depending on the voltage of the vertical gate, which controls the magnitude of the Bychkov–Rashba SOI.

The observation of AC oscillations in hole conduction, illustrating the effect of a spin transistor at a high temperature (T = 77 K), became possible due to the high degree of spin polarization of holes and the large time of their spin relaxation. This is due to the extremely small width of the silicon QW and its edge channels ensured by the properties of the limiting negative-U-barriers, which effectively suppress EEI.

## References

1. Wharam DA, Thornton TJ, Newbury R, Pepper M, Ahmed H, Frost JEF, Hasko EG, Peacock EC, Ritchie DA, Jones GAC. One-dimensional transport and the quantisation of the ballistic resistance. *J. Phys. C.* 1988;21(8): L209−L214.

2. Van Wees BJ, Van Houten H, Beenakker CWJ, Williamson JG, Kouwenhoven LP, Van der Marel D, Foxon CT. Quantized conductance of point contacts in a two-dimensional electron gas. *Phys. Rev. Lett*. 1988;60(9): 848−850.

3. Graham AC, Sawkey DL, Pepper M, Simmons MY, Ritchie DA. Energy-level pinning and the 0.7 spin state in one dimension: GaAs quantum wires studied using finite-bias spectroscopy. *Phys. Rev. B.* 2007;75(3): 035331.

4. Bagraev NT, Shelykh IA, Ivanov VK, Klyachkin LE. Spin depolarization in quantum wires polarized spontaneously in a zero magnetic field. *Phys. Rev. B.* 2004;70(15): 155315.
5. Bychkov YA, Rashba E I. Oscillatory effects and the magnetic susceptibility of carriers in inversion layers. *J. Phys. C.* 1984;17(33): 6039−6045.
6. Datta S, Das B. Electronic analog of the electro-optic modulator. *Appl. Phys. Lett.* 1990;56(7): 665−667.
7. Ghiasi TS, Kaverzin AA, Blah PJ, Van Wees BJ, Charge-to-Spin Conversion by the Rashba−Edelstein Effect in Two-Dimensional van der Waals Heterostructures up to Room Temperature. *Nano Lett.* 2019;19: 5959−5966.
8. Koch M, Keizer J., Pakkiam P, Keith D, House MG, Peretz E, Simmons MY, Spin read-out in atomic qubits in an all-epitaxial three-dimensional transistor. *Nature Nanotech.* 2019;14: 137–140.
9. Camenzind LC, Geyer S, Fuhrer A, Warburton RJ, Zumbühl DM, Kuhlmann AV. A hole spin qubit in a fin field-effect transistor above 4 kelvin. *Nat Electron*. 2022;5: 178–183.
10. Bhattacharyya K, Debnath D, Chatterjee A. Rashba effect on finite temperature magnetotransport in a dissipative quantum dot transistor with electronic and polaronic interactions. *Sci Rep.* 2023;13: 5500.
11. Johnson M, Silsbee RH. Coupling of electronic charge and spin at a ferromagnetic-paramagnetic metal interface. *Phys. Rev. B.* 1988;37(10): 5312−5325.
12. Meservey R, Paraskevopoulos D, Tedrow PM. Correlation between Spin Polarization of Tunnel Currents from 3d Ferromagnets and Their Magnetic Moments. *Phys. Rev. Lett.* 1976;37(13): 858−860.
13. Aronov AG, Lyanda-Geller YB. Spin-orbit Berry phase in conducting rings. *Phys. Rev. Letters.* 1993;70(3): 343−346.
14. Winkler R. Rashba spin splitting in two-dimensional electron and hole systems. *Phys. Rev. B.* 2000;62(7): 4245-4248.
15. Winkler R, Noh H, Tutuc E, Shayegan M. Anomalous Rashba spin splitting in two-dimensional hole systems. *Phys. Rev. B.* 2002;65(15): 155303.
16. Knap W, Skierbiszewski C, Zduniak A, Litwin-Staszewska E, Bertho D, Kobbi F, Robert JL, Pikus GE, Pikus FG, Iordanskii SV, Mosser V, Zekentes K, Lyanda-Geller YB. Weak antilocalization and spin precession in quantum wells. *Phys. Rev. B.* 1996;53(7): 3912−3924.
17. Awschalom DD, Loss D, Samarth N. *Semiconductor Spintronics and Quantum Computations*. Berlin: Springer; 2002.
18. König M, Tschetschetkin A, Hankiewicz EM, Sinova J, Hock V, Daumer V, Schäfer M, Becker CR, Buhmann H, Molenkamp LW. Direct Observation of the Aharonov-Casher Phase. *Phys. Rev. Lett.* 2006;96(7): 076804.
19. Bergsten T, Kobayashi T, Sekine Y, Nitta J. Experimental Demonstration of the Time Reversal Aharonov-Casher Effect. *Phys. Rev. Lett*. 2006;97(19): 196803.
20. Bagraev NT, Gehlhoff W, Klyachkin LE, Naeser A, Rykov S. Quantum-Well Boron and Phosphorus Diffusion Profiles in Silicon. *Defect and Diffusion Forum*. 1997;143−147: 10031008.
21. Bagraev NT, Grigoryev VY, Klyachkin LE, Malyarenko AM, MashkovVA, Rul NI. High-temperature quantum kinetic effect in silicon nanosandwiches. *Low Temperature Physics*. 2017;43(1): 132-142.
22. Bagraev NT, Galkin NG, Gehlhoff W, Klyachkin LE, Malyarenko AM. Phase and amplitude response of the '0.7 feature' caused by holes in silicon one-dimensional wires and rings. *J. Phys.: Condens. Matter*. 2008;20(16): 164202.

23. Klyachkin LE, Bagraev NT, Malyarenko AM. Macroscopic quantum effects of electromagnetic induction in silicon nanostructures. *Mater. Phys. Mech*. 2022;50(2): 252−265.
24. Nitta J, Meijer FE, Takayanagi H. Spin-interference device. *Appl. Phys. Lett*. 1999;75: 695−697.
25. Shelykh IA, Galkin NG, Bagraev NT. Quantum splitter controlled by Rashba spin-orbit coupling. *Phys. Rev. B*. 2005;72(23): 235316.
26. Zitouni O, Boujdaria K, Bouchriha H. Band parameters for GaAs and Si in the 24-k p model. *Semicond. Sci. Technol*. 2005;20(9): 908−911.
27. Bagraev NT, Mashkov VA. Danilovsky EY, Gehlhoff W, Gets DS, Klyachkin LE, Kudryavtsev AA, Kuzmin RV. Malyarenko AM, Romanov VV. EDESR and ODMR of Impurity Centers in Nanostructures Inserted in Silicon Microcavities. *Appl Magn Reson*. 2010;39: 113−135.
28. Geim AK, Novoselov KS. The rise of graphene. *Nature Mater*. 2007;6(3): 183−191.
29. Shelykh IA, Bagraev NT, Galkin NG, Klyachkin LE. Interplay of h/e and h/2e oscillations in gate-controlled Aharonov-Bohm rings. *Phys. Rev. B*. 2005;71(11): 113311.
30. Khaetskii AV, Nazarov YV. Spin relaxation in semiconductor quantum dots. *Phys. Rev. B*. 2000;61(19): 12639.

## THE AUTHORS

**Klyachkin L.E.**
e-mail: leonid.klyachkin@gmail.com

**Bagraev N.T.**
e-mail: bagraev@mail.ioffe.ru

**Malyarenko A.M.**
e-mail: annamalyarenko@mail.ru